land

MDPI

Article

Carbon Emission Status and Regional Differences of China: High-Resolution Estimation of Spatially Explicit Carbon Emissions at the Prefecture Level

Jinwei Guo [1,2], Yanbing Qi [1,*], Jiaqi Luo [1], Guohong Du [1], Jingyan Sun [1], Xin Wei [3,*] and Mukesh Kumar Soothar [1]

[1] College of Natural Resources and Environment, Northwest A&F University, Yangling, Xianyang 712100, China; guojinwei@nwafu.edu.cn (J.G.); luojiaqi@nwafu.edu.cn (J.L.); guohongdu@nwafu.edu.cn (G.D.); sjy@nwafu.edu.cn (J.S.); kumarmk@nwafu.edu.cn (M.K.S.)
[2] Department of Pharmacy, Changzhi Medical College, Changzhi 046000, China
[3] College of Humanities & Social Development, Northwest A&F University, Yangling, Xianyang 712100, China
* Correspondence: ybqi@nwsuaf.edu.cn (Y.Q.); wx@nwsuaf.edu.cn (X.W.)

Abstract: There are disagreements regarding the accuracy of estimation and spatial distribution of carbon emissions in China. It is of great significance to estimate a more detailed carbon emission inventory for China and analyze the carbon emission characteristics of different regions. This study comprehensively estimated carbon dioxide and methane emissions (and their spatial distributions) across eight carbon-emitting sectors in 360 prefecture-level cities in China in 2020. The results indicated that total carbon emissions in China amounted to 146.00 × 10^8 t, with carbon dioxide and methane accounting for 95.87% and 4.13%, respectively. The industrial sector was the main source of carbon emissions, accounting for 75.42% of the total. The North China Plain, the Northeast Plain, and the Sichuan Basin were identified as the carbon emission hotspot areas with the most intensive carbon emission densities. Among the clustered four carbon emission zones based on carbon emission density and economic carbon intensity, the High Carbon Emission Density and High Economic Carbon Intensity zones accounted for 41.73% of total carbon emissions. To achieve carbon neutrality, it is essential to devise emission reduction strategies for specific areas by thoroughly considering spatially explicit variation at the prefecture level, with a focus on primary carbon-emitting cities and sectors.

Keywords: carbon emission estimation; prefecture level; carbon emission sources; carbon emission zoning; China

Academic Editor: Marko Scholze

Received: 6 January 2025
Revised: 24 January 2025
Accepted: 28 January 2025
Published: 30 January 2025

Citation: Guo, J.; Qi, Y.; Luo, J.; Du, G.; Sun, J.; Wei, X.; Soothar, M.K. Carbon Emission Status and Regional Differences of China: High-Resolution Estimation of Spatially Explicit Carbon Emissions at the Prefecture Level. *Land* **2025**, *14*, 291. https://doi.org/10.3390/land14020291

1. Introduction

Increasing carbon emissions from human activities have been regarded as the major contributor to global climate change [1,2], posing significant challenges to the sustainable development of human society and the environment [3]. In the past decades, China has experienced rapid economic growth, industrialization, and urbanization, resulting in substantial energy consumption and carbon emissions [4–6], making China the world's largest emitter of carbon. In response to the challenges posed by global climate change, the Chinese government has implemented a series of significant measures, i.e., improving energy efficiency, developing renewable energy sources, and advocating green travel [7–9], with the objective of reducing carbon emissions and promoting sustainable

development. Nevertheless, it is worth acknowledging that despite the significant progress achieved, China continues to be one of the world's foremost contributors to carbon emissions [6,10].

China's carbon emissions originate from multiple sources. In the Guidelines for Compiling Provincial Greenhouse Gas Inventories issued by the Department of Climate Change under the National Development and Reform Commission in 2010, carbon emissions were categorized into several sectors, including agriculture, industry, livestock farming, construction, transportation, tertiary industry, residential living, and waste disposal. These eight sectors generally represent the overall carbon emission levels across regions in China. However, current research on China's carbon emissions often focuses on several specific carbon-emitting sectors, such as agriculture [11,12], construction [13], residential living [14], industry [15,16], transportation [17], and food [18]. In addition, scholars have usually only estimated carbon dioxide (CO_2) emissions from fossil fuel consumption and industrial production processes [19–22] but have ignored methane (CH_4) emissions. Differences in focus have led to certain differences in estimates of China's carbon emissions, such as those reported by Kong et al. (2022) (121.92×10^8 t in 2019) [21], the International Energy Agency (IEA) (100.53×10^8 t in 2020), and the China City Greenhouse Gas Working Group (CCG) (127.3×10^8 t in 2020). Therefore, there is a pressing need to consider more potential sources of carbon emissions in order to accurately assess China's carbon emissions and to provide data support for the early realization of carbon peaking and carbon neutrality in China.

High-resolution networked data are the foundation for accurately identifying carbon emission hotspots and proposing targeted emission reduction strategies [23]. Several studies have employed data for population density [24] and nighttime lights [25] to model the spatial distribution of carbon emissions. However, it is important to note that these datasets are better suited for quantifying carbon emissions linked to population density and electricity usage but may not accurately capture emissions from other sources of energy consumption, such as industrial energy consumption [26]. Land use plays a crucial role in carbon emissions and mitigation efforts [27], as land use patterns directly influence energy consumption, transportation networks, industrial locations, and population distribution. Changes in land use patterns and structures can significantly alter energy consumption patterns, thereby impacting carbon emissions [28]. Optimizing land-use structures, such as reallocating industrial land, could serve as an important tool for reducing carbon emissions [29]. While some researchers have provided high-resolution (50–1000 m) carbon emission data at the county level [30] or city level [31–35], comprehensive high-resolution emission data covering the entirety of China remains scarce. Cai et al. (2018) developed the China High-Resolution Emission Database (CHRED) that incorporates both point source and gridded emission data at spatial resolutions of 1 km and 10 km [19]. This dataset significantly improved the precision and accuracy of regional emission estimation, and demonstrated clear advantages in pinpointing carbon emission hotspots. However, further improving spatial resolution is essential for effective carbon emission management, as it allows for the identification of carbon emission patterns at finer scales. Such advancements can support more accurate and localized decision-making, including the development of emission reduction strategies tailored to specific land use types or addressing hotspot issues in industrial zones, where many factories are located just a few hundred meters from residential areas. High-resolution data also facilitate dynamic monitoring of land use changes and their carbon impacts, providing valuable insights for sustainable urban planning and industrial regulation.

Therefore, the primary objective of this study is to achieve high-precision accounting and accurate spatial identification of carbon emissions in China by integrating multi-source data with comprehensive analytical methods. Furthermore, the study aims to

examine the spatial patterns and characteristics of carbon emissions, offering insights into their dynamics and distribution across different regions. This approach not only enhances the understanding of regional emission trends but also provides a scientific foundation for formulating highly targeted emission reduction strategies, thereby supporting more refined and effective carbon emission management. Given this context, the three primary objectives of this study were to (1) conduct detailed carbon emissions accounting on a prefecture-level city basis, (2) provide high-resolution (500 m) carbon emissions data for China, and (3) determine carbon emission sources across different regions in order to present tailored emission reduction recommendations. To achieve these objectives, we used statistical data at the prefecture-level scale that encompassed agriculture, industry, livestock farming, construction, transportation, tertiary industry, residential living, and waste disposal to compute the CO_2 and CH_4 emissions in 360 prefecture-level cities in China for 2020. By leveraging high-resolution spatial data, including Point of Interest (POI) data, land-use data, road data, population density data, and nighttime light data, we were able to determine the spatial distribution of carbon emissions in order to achieve relatively comprehensive and high-resolution (500 m) carbon emissions data. The ultimate research objectives were to identify carbon emission hotspots and propose corresponding emission reduction suggestions for different regions in order to provide a theoretical basis for the precise implementation of carbon emission reduction strategies in specific regions of China in the future. The findings of this study provide detailed data support for the development of scientifically sound and rational carbon reduction policies, enabling their precise implementation. Furthermore, the study offers valuable insights for more effective monitoring of carbon emissions across regions, particularly in improving the management of key areas and industries. The results contribute to the Sustainable Development Goals (SDGs), including the "Climate Action" goal, by accurately assessing carbon emissions and supporting the formulation of effective reduction strategies to address climate change. Additionally, in relation to the "Sustainable Cities and Communities" goal, the study provides data-driven insights to guide urban planning and management, fostering the green and low-carbon development of cities.

2. Materials and Methods

2.1. Study Area

We chose the mainland of China as the study area due to the unavailability of the necessary statistical data for Xizang, Hong Kong, Macau, and Taiwan. A total of 360 cities across 30 provinces in the study area were selected for calculating carbon emissions (Figure 1). Among the 360 cities, there were 287 prefecture-level cities, 30 autonomous prefectures, four municipalities directly under the direction of the central government, and 39 other cities directly administered by provincial governments, collectively referred to hereafter in this paper as prefecture-level cities for the sake of simplicity.

Figure 1. Study area in China.

2.2. Data Sources

Two types of data were employed in this study: non-spatial data and spatial data. The non-spatial data primarily originated from official statistical publications issued by the Chinese government and provincial-level authorities. These publications are highly authoritative and systematically compile comprehensive data related to China and its respective provinces. Such data are crucial for accurately analyzing economic activities and their associated carbon emissions across diverse regions. Furthermore, the data obtained from these sources are collected through official statistical websites, ensuring both its accuracy and representativeness for carbon emission analysis. Non-spatial data included energy consumption data (sourced from the China Energy Statistical Yearbook) [36]; population data (sourced from the Seventh National Population Census of China) [37]; year-end livestock inventory, raw coal production, industrial product output, agricultural input, rice cultivation area, grain production, operating costs of various industrial sectors, construction area, road mileage, disposable income of residents, total output of the tertiary sector (sourced from Provincial Statistical Yearbooks and Prefecture-level City Statistical Yearbooks on the government websites of various provinces and cities); and sewage treatment volume and solid waste disposal volume (sourced from the China Environmental Statistical Yearbook) [38]. All non-spatial data for this study were collected in 2020. The spatial data constituted road data (encompassing expressways, national highways, provincial roads, urban primary roads, urban secondary roads, urban tertiary roads, and urban quaternary roads) [39]; land use data with a spatial resolution of 30 m [39]; nighttime light data with a spatial resolution of 500 m [40]; and WorldPop population distribution data with a spatial resolution of 100 m [41]. The map of China was obtained from the official website of the Ministry of Natural Resources of China in 2022 [42]. Points of Interest (POI) data, representing geospatial vector points based on mobile devices and location services, contain semantic information that cannot be derived from satellite images [43]. Different types of POI data reflect the spatial distribution of various carbon emissions, addressing the limitations of using remote sensing data to monitor carbon emissions in

complex urban environments. As a result, POI data are widely used in carbon emission estimation [44]. Therefore, we obtained POI data from various industries using the Gaode Maps API interface technology from Gaode Maps, including 1,837,202 entries of industrial data, 7238 entries of cement production plants, 6407 entries of steel production factories, 46,911 entries of large-scale livestock farms, 662 entries of wastewater treatment plants, and 1191 entries of waste disposal facilities. The industrial POI data were categorized into 40 carbon-emitting sectors based on industrial classification standards from the Provincial Statistical Yearbook (sourced from the government websites of various provinces) (Table A1). All of the spatial data were collected in 2020. Considering that the nighttime light data exhibit a native resolution of 500 m, in order to preclude potential errors that might arise from resampling to higher resolution data, all spatial data employed in this study were uniformly resampled to a consistent spatial resolution of 500 m.

2.3. Estimating and Spatializing Carbon Emissions

Two main steps comprised the process used in this study: 1. estimating carbon emissions; 2. spatializing carbon emissions.

2.3.1. Estimating Carbon Emissions

Our first objective was to compute the carbon emissions from 17 different sources, encompassing the eight carbon-emitting sectors of agriculture, industry, livestock farming, construction, transportation, tertiary sector, residential living, and waste disposal (Table 1). Given that the statistical yearbooks of prefecture-level cities contain energy consumption data for only a limited number of major energy sources, we utilized provincial-level energy consumption data to calculate carbon emissions. The majority of other non-spatial data was at the prefecture-level city, with only a portion being at the provincial level. In the end, different proxy data varying by sector and data type were selected to distribute carbon emissions calculated from provincial-level data to individual prefecture-level cities (Table A2). Due to the unavailability of location data for waste disposal facilities in some prefecture-level cities, carbon emissions resulting from waste disposal were calculated and allocated at the provincial level.

Table 1. Types, sources, and associated sectors of carbon emissions.

Associated Sector	Carbon Emission Source	Carbon Emission Type
Agriculture	Agricultural Energy Consumption	CO_2
	Agricultural Input Materials	CO_2
	Methane Emissions from Rice Cultivation	CH_4
Livestock Farming	Livestock Manure Fermentation	CH_4
	Livestock Enteric Management	CH_4
Industry	Coal Mining	CH_4
	Industrial Energy Consumption	CO_2
	Industrial Production Processes	CO_2
Construction	Construction Energy Consumption	CO_2
Transportation	Transportation Energy Consumption	CO_2
Residential Living	Urban Residential living Energy Consumption	CO_2
	Rural Residential living Energy Consumption	CO_2
Waste Disposal	Sewage Treatment	CH_4
	Waste Incineration	CO_2
	Waste Landfilling	CH_4
Tertiary Sector	Wholesale, Retail, and Catering Services Energy Consumption	CO_2

Other Energy Consumption	CO_2

These calculations accounted for two greenhouse gases: CO_2 and CH_4. The equations for calculating carbon emissions are shown in Equation (1). All calculation results were ultimately converted into CO_2 emissions and aggregated.

$$C = \sum (C_{cdi} + C_{mek}) = \sum (Q_i \times Z_i + Q_k \times Z_k \times 21) \quad (1)$$

where C represents the total carbon emissions; C_{cdi} represents the carbon dioxide emissions of the ith type; C_{mek} represents the methane emissions of the kth type (converted to carbon dioxide equivalent); Q_i and Q_k represent the quantities of the ith and kth related resource types, while Z_i and Z_k represent the carbon emission coefficients of the ith and kth source types, respectively. The conversion factor of 21 means that 1-tone CH_4 is equivalent to 21-tone CO_2 equivalent [45]. The carbon emission coefficients for different sources are shown in Table A3.

2.3.2. Spatializing Carbon Emissions

Our second objective was to allocate carbon emissions spatially. Diverse spatial allocation methods were adopted based on data characteristics. For point data, carbon emissions from the same source were evenly distributed among various POIs. For linear and areal data, different proxy data were selected as weights based on the unique characteristics of different carbon emission types, and then carbon emissions were allocated to specific grid units with prefecture-level cities as the basic units (Equations (2) and (3)). Additionally, for areal data, different carbon emissions were assigned to different land use types (Table A4).

$$C_g = \sum C_{gi} = C_{cityi} \times W_{gi} \quad (2)$$

$$W_{gi} = Z_{gi} / Z_{cityi} \quad (3)$$

where C_g represents the carbon emissions of grid unit g; C_{gi} represents the carbon emissions of type i on grid unit g; C_{cityi} represents the total carbon emissions of type i for the respective prefecture-level city; W_{gi} represents the weight assigned to type i carbon emissions for grid unit g; Z_{gi} represents to the proxy data value for type i carbon emissions on grid unit g; and Z_{cityi} represents the summation of proxy data values for type i carbon emissions within the same prefecture-level city.

2.4. Carbon Emission Zoning

Our final objective was to divide all 360 prefecture-level cities into different zones based on their carbon emission characteristics and propose carbon reduction recommendations. Carbon emission density is defined as the amount of CO_2 per land area [46], and economic carbon intensity is defined as the amount of CO_2 per unit of gross domestic product (GDP) [47]. The prefecture-level cities were zoned into four zones based on carbon emission density and economic carbon intensity: low carbon emission density and low economic carbon intensity zone (LD-LI), low carbon emission density and high economic carbon intensity zone (LD-HI), high carbon emission density and high economic carbon intensity zone (HD-HI), and high carbon emission density and low economic carbon intensity zone (HD-LI). The LD HD means the carbon emission density of prefecture-level cities is less or more than that of the average in China, and LI (HI) means the economic carbon intensity of prefecture-level cities is less or more than that of the average in China.

2.5. Kernel Density Method

The kernel density method directly reflects the density of point data within a certain area [48]. The kernel density method was used to detect the spatial distribution characteristics of carbon emissions in China after the spatial data were converted into point data. The resolution of the kernel density method was 500 m, and the specified search radius was 10 km.

3. Results

3.1. Carbon Emission Status in China

Total carbon emissions in China amounted to 146.00 × 10^8 t in 2020 (Table 2), among which CO_2 contributed 139.97 × 10^8 t (accounting for 95.87% of the total carbon emissions, and CH_4 accounting for only 4.13%). Industry was the dominant sector among the eight designated carbon-emitting sectors, contributing 110.12 × 10^8 t (accounting for 75.42% of the total). Carbon emissions from residential living, transportation, tertiary sector, and agriculture accounted for 7.44%, 5.16%, 4.89%, and 3.82%, respectively, of the total. The highest contributor to CO_2 emissions was industry (accounting for 77.43% of the total CO_2 emissions). Livestock farming and industry had the largest CH_4 emissions (accounting for 36.98% and 28.86%, respectively, of total CH_4 emissions.

Table 2. Carbon emissions from different sources in 2020 (10^8 t).

Carbon Emission Source	Carbon Emissions		
	Total	**CO_2**	**CH_4**
Agriculture	5.58	4.24	1.34
Livestock Farming	2.23	0	2.23
Industry	110.12	108.38	1.74
Construction	1.48	1.48	0
Transportation	7.53	7.53	0
Residential Living	10.85	10.85	0
Tertiary Sector	7.14	7.14	0
Waste Disposal	1.07	0.35	0.72
Total	146.00	139.97	6.03

Significant spatial variation in carbon emissions in China was detected, with higher emissions in the southeastern area than in the northwestern area (Figure 2a). Based on the kernel density analysis, the identified high carbon emission aggregation areas were the North China Plain (including Beijing, Tianjin, Hebei, Henan, Shandong, Anhui, and Jiangsu), the Northeast Plain (including Heilongjiang, Jilin, Liaoning, and eastern Inner Mongolia), and the Sichuan Basin (including eastern Sichuan and western Chongqing) (Figure 2b). The five highest carbon-emitting provinces were Hebei (16.72 × 10^8 t), Shandong (13.65 × 10^8 t), Jiangsu (11.23 × 10^8 t), Liaoning (7.62 × 10^8 t), and Inner Mongolia (7.11 × 10^8 t), all five of which accounted for 38.57% of the total carbon emissions in China. The five provinces with the lowest carbon emissions were Chongqing, Ningxia, Beijing, Qinghai, and Hainan, all five of which contributed to only 4.65% of the total national carbon emissions.

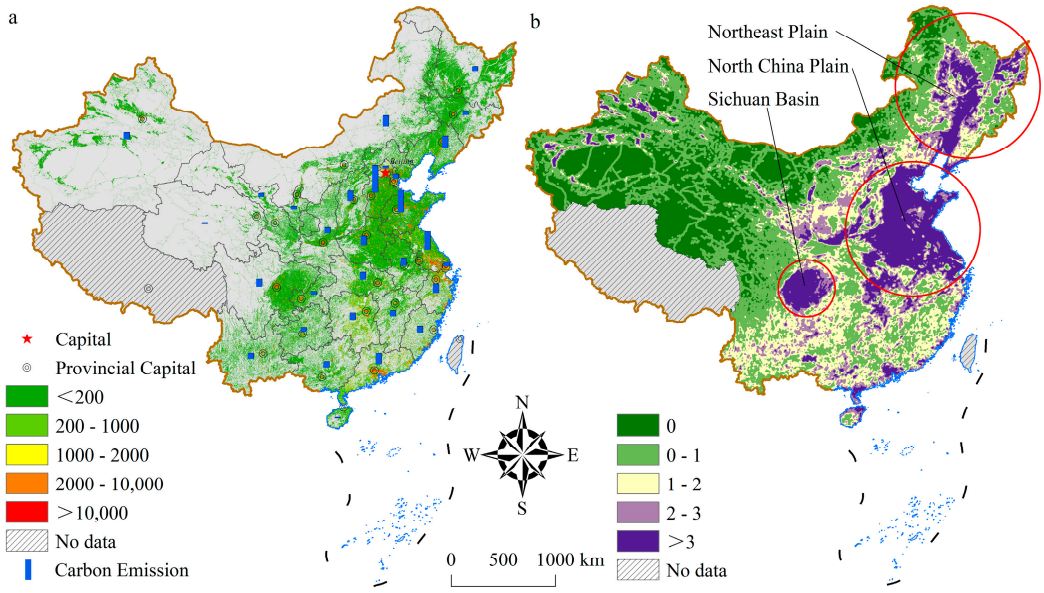

Figure 2. Spatial distribution characteristics of carbon emissions in China in 2020: (**a**) spatially explicit carbon emissions (t/grid cell); (**b**) kernel density analysis.

As with the spatial distribution trends of total carbon emissions for the entire county, the carbon emissions from the selected eight carbon-emitting sectors were higher in southeastern China than in northwestern China (Figure 3). The areas with higher carbon emissions from the industrial sector were located in Hebei, Liaoning, Shanxi, and Inner Mongolia, provinces that are famous for steel production and coal mining. Areas with more intensive carbon emissions from residential living were mainly located in Shandong, Henan, Hebei, Jiangsu, and Anhui, where population densities were higher. Carbon emissions from transportation and agriculture were more concentrated, while carbon emissions from tertiary industry, construction, and waste disposal were relatively dispersed. Carbon emissions from livestock farming were more concentrated in the North China Plain, but higher emissions were produced in the southwest.

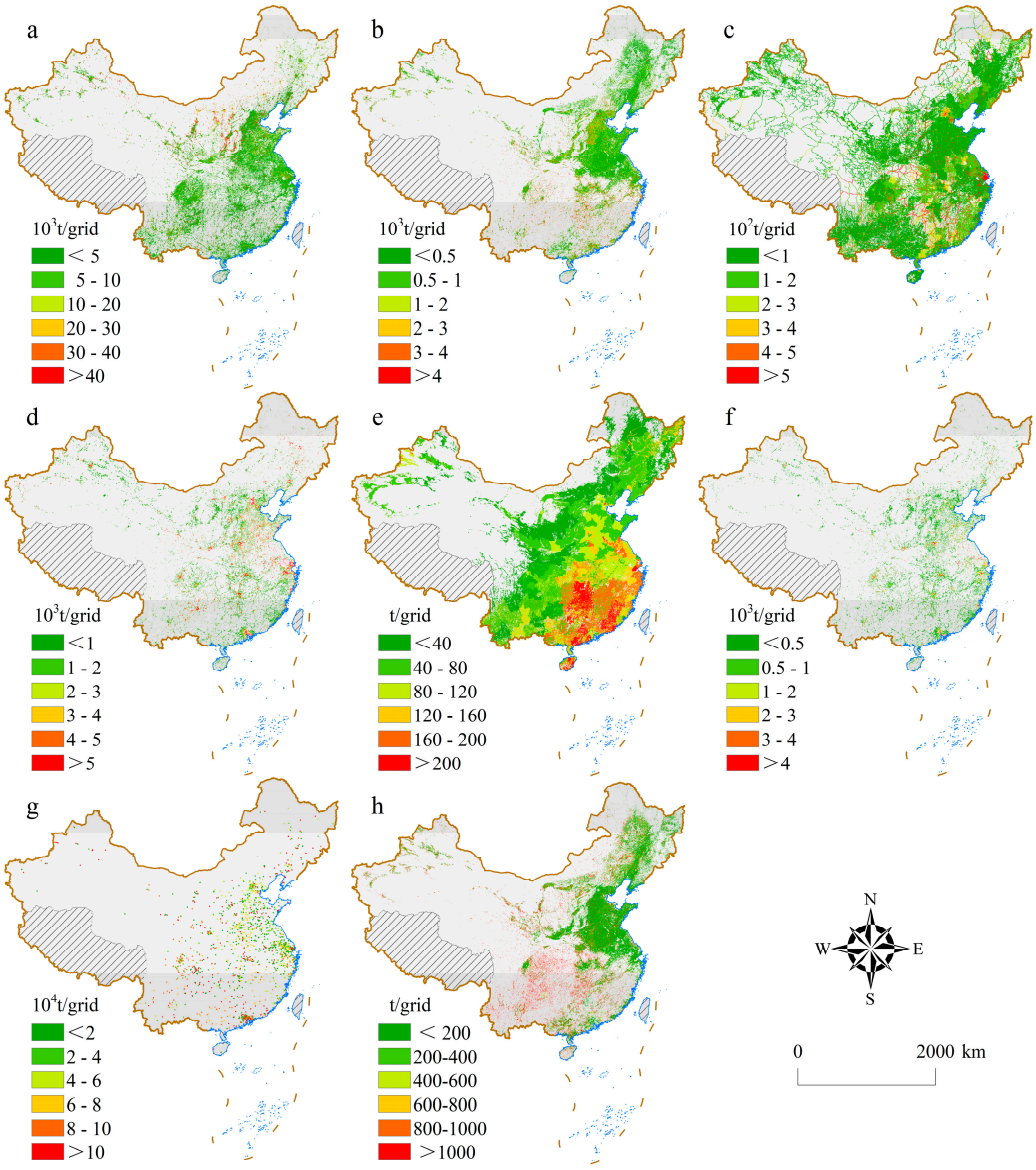

Figure 3. Spatially explicit carbon emissions from eight carbon-emitting sectors in China in 2020: (**a**) industry; (**b**) residential living; (**c**) transportation; (**d**) tertiary sector; (**e**) agriculture; (**f**) construction; (**g**) waste disposal; (**h**) livestock farming.

The industry sector accounted for more than 50% of total carbon emissions from most of the provinces except Beijing and Heilongjiang (Figure 4). Specifically, the industry sector contributed to more than 70% of the total carbon emissions in 17 provinces, and the top three industrial carbon-emitting provinces were Ningxia (88.56%), Hebei (88.08%), and Shanxi (85.84%). It is worth noting that residential living and transportation carbon emissions also accounted for a large proportion of carbon emissions in dense population areas such as Beijing (25.22%), Heilongjiang (15.85%), and Guangdong (10.00%). The top three transportation carbon-emitting provinces were Shanghai (17.78%), Beijing (16.37%), and Hainan (12.58%), and the top three tertiary industry carbon-emitting provinces were Beijing (32.29%), Guizhou (16.72%), and Shanghai (11.79%). Not surprisingly, the largest agricultural carbon-emitting province was Heilongjiang (13.30%) due to it being the main grain-producing area of China, followed by Hainan (10.45%) and Hunan (9.87%).

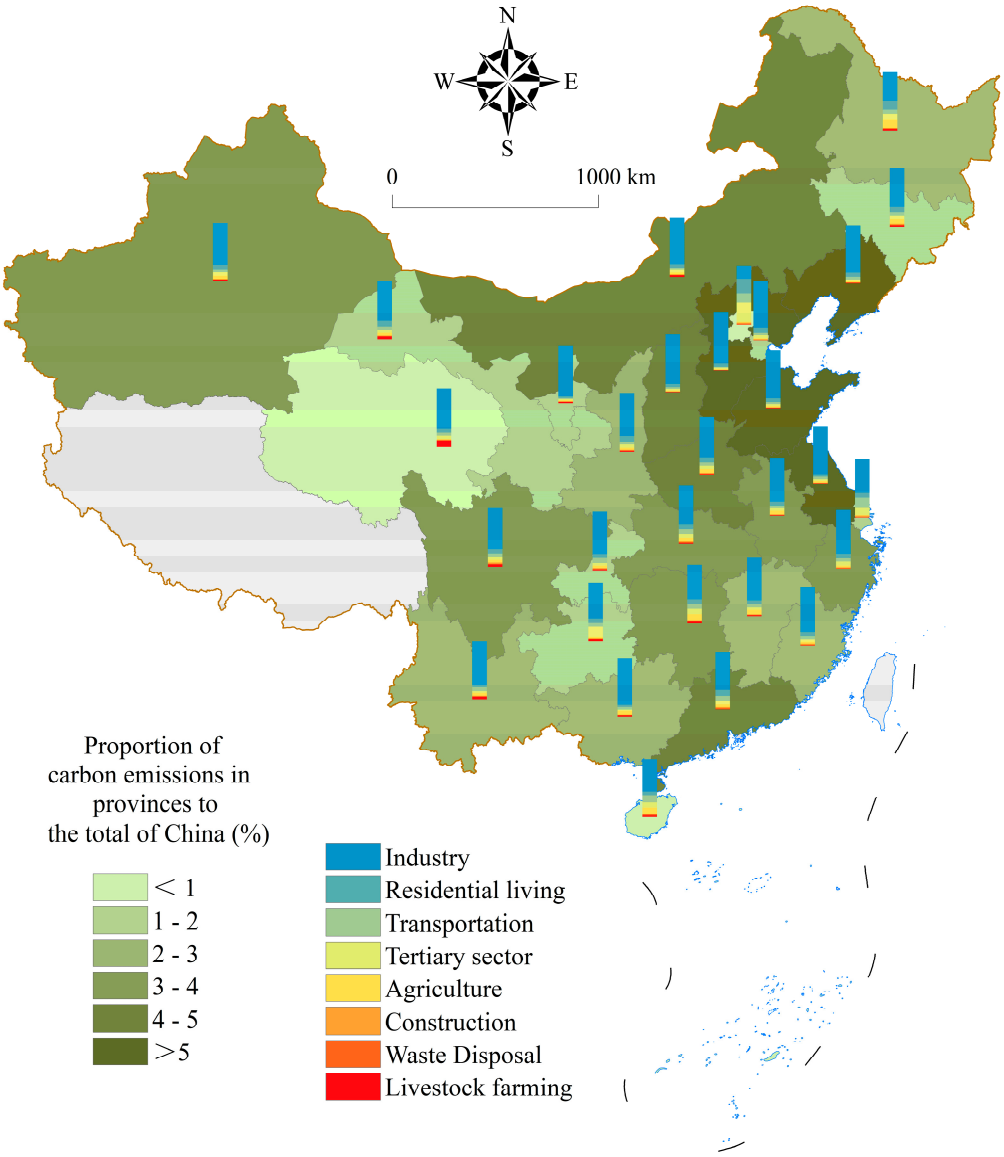

Figure 4. The proportion of total carbon emissions in China coming from each province (green shading of provinces) and the proportion of total carbon emissions in each province attributed to each carbon-emitting sector (segmented color bars in each province).

3.2. Carbon Emission Characteristics at Prefecture-Level Cities

The industry sector accounted for more than 50% of carbon emissions from the 309 prefecture-level cities. Specifically, the industry sector contributed to more than 80% of the carbon emissions in 83 prefecture-level cities mainly located in the north of China (Figure 5a). The carbon emissions from residential living and tertiary sector showed obvious agglomeration in Heilongjiang and Guizhou, respectively (Figure 5b,d). The 36 cities with transportation carbon emissions exceeding 15% were mainly located in the southwest, southern coastal, and northeastern regions (Figure 5c). For agriculture, the 27 cities with carbon emissions exceeding 15% were mainly located in Heilongjiang, Xinjiang, Henan, and Hainan (Figure 5e). Relative to other sectors, carbon emissions from construction, waste disposal, and livestock farming accounted for a smaller proportion of the total carbon emissions in each prefecture-level city (Figure 5f–h).

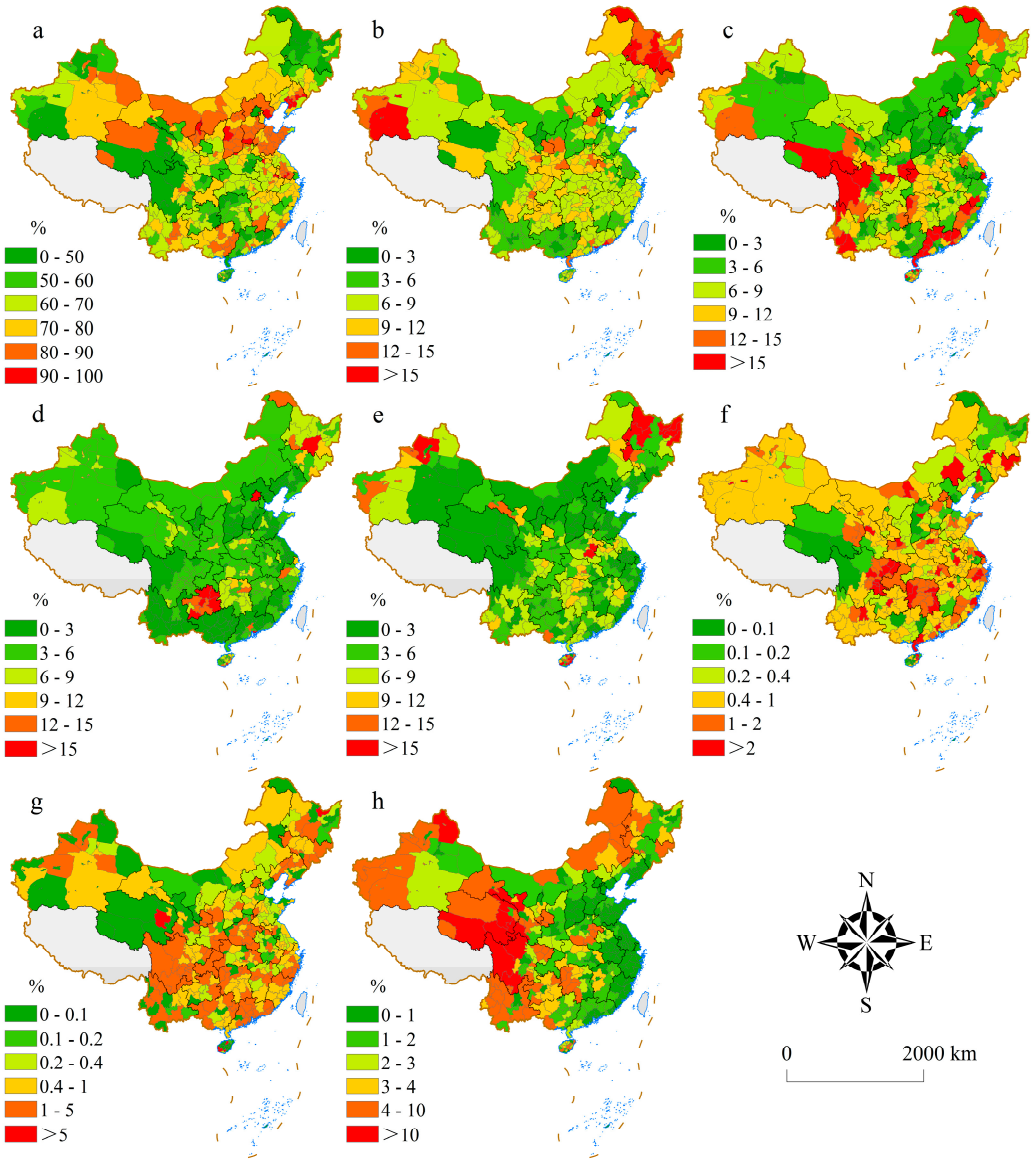

Figure 5. Proportions of total carbon emissions from eight carbon-emitting sectors in China: (**a**) industry; (**b**) residential living; (**c**) transportation; (**d**) Tertiary sector; (**e**) Agriculture; (**f**) Construction; (**g**) Waste disposal; (**h**) Livestock farming.

As shown in Figure 6a, there were 76 cities with carbon emissions exceeding 60 million tons that contributed carbon emissions of 83.72×10^8 t (Table 3), accounting for 57.34% of the total carbon emissions in China. The top five carbon-emitting prefecture-level cities were Tangshan with 502.39 million tons, Tianjin with 282.35 million tons, Shanghai with 260.14 million tons, Suzhou with 245.35 million tons, and Handan with 233.82 million tons, accounting for a total of 10.44% of the total carbon emissions in China.

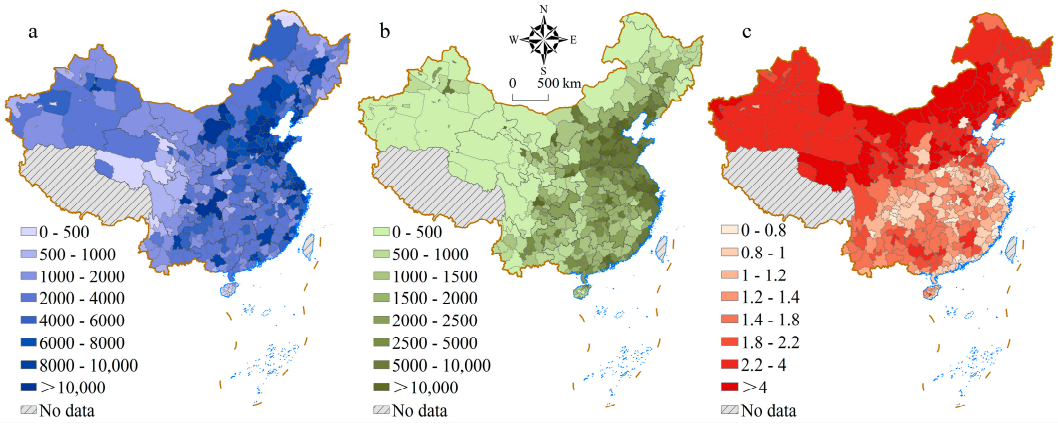

Figure 6. Carbon emission characteristics of prefecture-level cities in China: (**a**) total carbon emissions (10^4 t); (**b**) carbon emission density (t/km^2); (**c**) economic carbon intensity (t/10^4 RMB).

Table 3. Number of prefecture-level cities and total carbon emissions for different levels of total carbon emissions, carbon emission density, and carbon emission intensity in China.

Classification		Number of Prefecture-Level Cities	Total Carbon Emissions (10^8 t)
Total carbon emissions (10^4t)	0–500	34	0.77
	500–1000	31	2.34
	1000–2000	76	11.35
	2000–4000	109	31.95
	4000–6000	34	15.88
	6000–8000	25	17.32
	8000–10,000	26	23.48
	>10,000	25	42.91
Carbon emission density (t/km^2)	0–500	46	5.74
	500–1000	47	8.41
	1000–1500	46	9.84
	1500–2000	42	11.91
	2000–2500	23	7.92
	2500–5000	62	21.99
	5000–10,000	53	34.25
	>10,000	41	45.94
Carbon emission intensity (t/10^4 RMB)	0.0–0.8	34	15.39
	0.8–1.0	46	15.55
	1.0–1.2	37	13.67
	1.2–1.4	42	15.86
	1.4–1.8	50	15.37
	1.8–2.2	30	14.41
	2.2–4.0	79	28.02
	>4.0	42	27.73

Significant spatial variation in carbon emission density in China was detected, with higher carbon emission density in the southeastern region than in the northwestern region (Figure 6b). Ninety-four cities had carbon emission densities exceeding 5000 t/km^2, contributing a total carbon emission of 80.19 × 10^8t and accounting for 54.92% of the total carbon emissions in China. The top five carbon emission density prefecture-level cities were Wuxi (3.96 × 10^4 t/km^2), Tangshan (3.64 × 10^4 t/km^2), Dongguan (3.55 × 10^4 t/km^2),

Shenzhen (3.46 × 10^4 t/km^2), and Shanghai (3.17 × 10^4 t/km^2), accounting for total carbon emissions of 7.53%.

Eighty-one cities had carbon emission intensities exceeding 3 t/10^4 RMB (Figure 6c), contributing a total carbon emission of 42.63 × 10^8 t and accounting for 29.20% of the total carbon emissions in China. The top five economic carbon intensity prefecture-level cities were Hainan Tibetan Autonomous Prefecture (11.54 t/10^4 RMB), Benxi (7.28 t/10^4 RMB), Tangshan (6.97 t/10^4 RMB), Wuhai (6.80 t/10^4 RMB), and Shizuishan (6.68 t/10^4 RMB), accounting for total carbon emissions of 4.39%.

The carbon emissions of prefecture-level cities gradually decreased from the city center to the periphery, but different spatial distribution characteristics in different cities were shown based on the degree of urban development (Figure 7). By utilizing high-resolution data, the localized patterns of carbon emissions in cities with varying levels of development can be accurately identified patterns that would otherwise be obscured in coarse-resolution analyses. For instance, in super-first-tier cities such as Shanghai and Shenzhen, high carbon emission areas were not only larger but also more spatially concentrated, reflecting dense industrial and commercial activities. In contrast, in first-tier cities like Dongguan, Suzhou, and Tianjin, as well as the second-tier city Wuxi, high-emission areas were moderately distributed, highlighting a mix of urban and peripheral industrial zones. In third-tier cities, such as Tangshan and Handan, the areas of high carbon emissions were smaller and scattered, often concentrated in specific industrial hubs or county capitals.

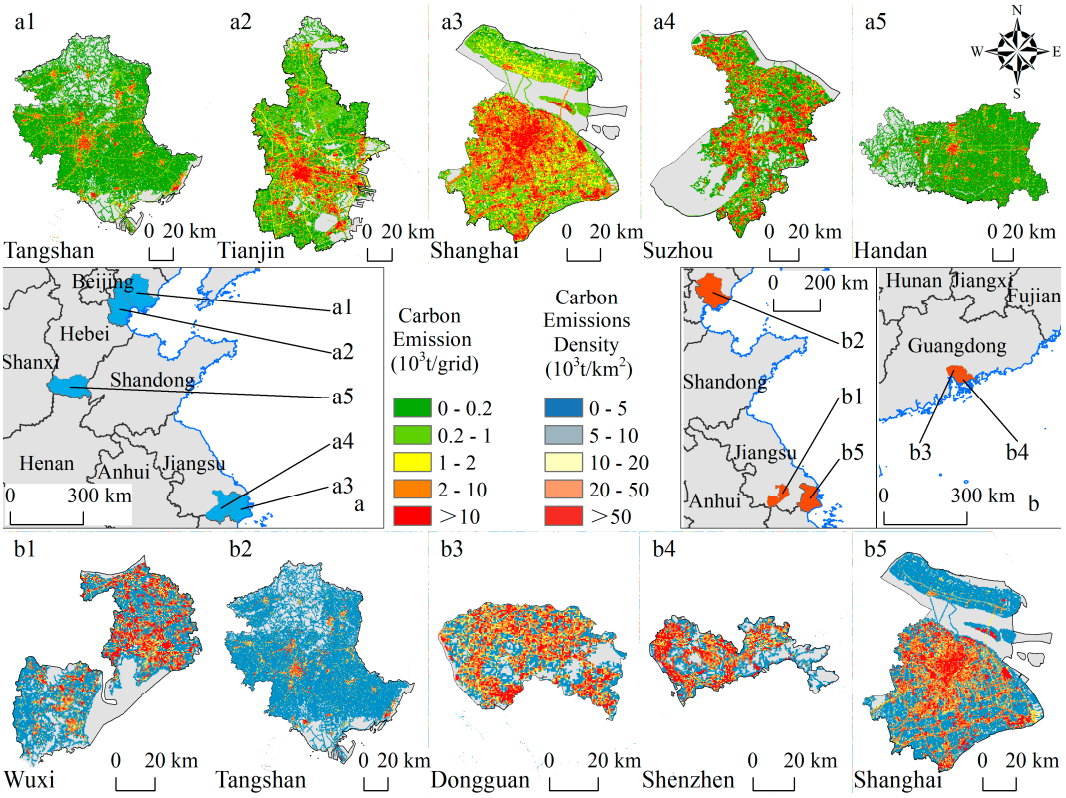

Figure 7. Positions and spatial distribution of the top five prefecture-level cities with the highest carbon emissions (**a**, **a1**–**a5**) and the top five prefecture-level cities with the highest carbon emission densities (**b**, **b1**–**b5**) in China.

3.3. Characteristics of Carbon Emissions in Different Zones

The average carbon emission density for China in 2020 was 1765.81 t/km^2, with an average economic carbon intensity of 1.44 t/10^4 RMB. Therefore, this study divided China

into four zones (Figure 8a). The four zones exhibited significant differences in spatial concentrations of emission characteristics, with the LD-LI zone predominantly situated in southern China (including 58 cities), the LD-HI zone located in northern China (including 103 cities), and the HD-LI and HD-HI zones primarily located in eastern China, distinctly divided along a north-south axis (including 109 and 90 cities, respectively). There were also significant differences in carbon emission values among the four regions, with the HD-HI zone having the highest carbon emissions and accounting for 41.73% of the total carbon emissions, while the LD-LI zone contributed to only 5.62% of total carbon emissions (Figure 9a). In addition, there were significant discrepancies in average carbon emission density between the LD zone (411.61–1002.07 t/km^2) and the HD zone (5200.48–6377.09 t/km^2), as well as in average economic carbon intensity between the LI zone (0.86–1.11 t/10^4 RMB) and HI zone (2.45–2.88 t/10^4 RMB) (Figure 9b,c).

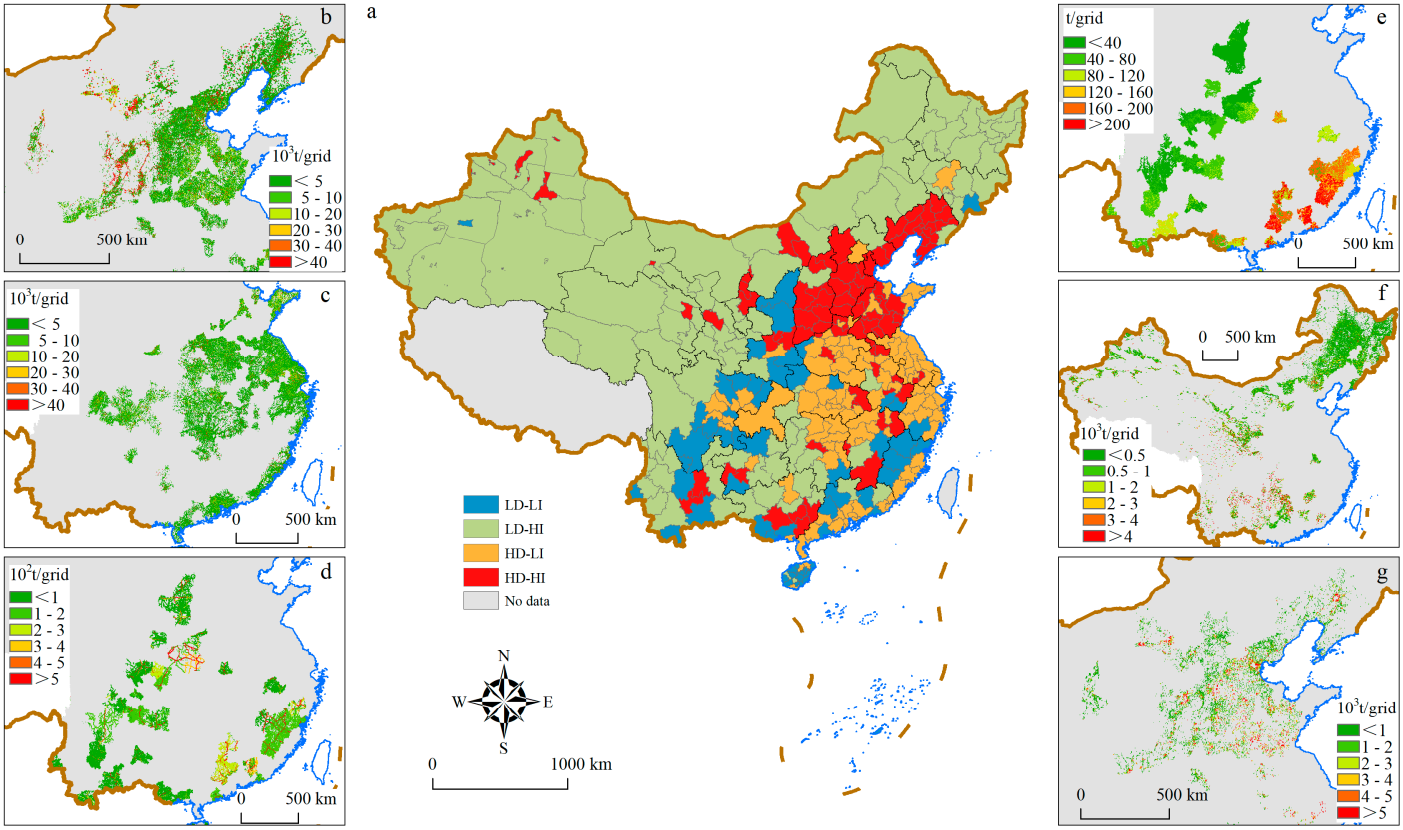

Figure 8. Carbon emission zones in China: (**a**) spatial distribution of four carbon emission zones; (**b**) industrial carbon emissions in the HD-HI zone; (**c**) industrial carbon emissions in the HD-LI zone; (**d**) transportation carbon emissions in the LD-LI zone; (**e**) agriculture carbon emissions in the LD-LI zone; (**f**) industrial carbon emissions in the LD-HI zone; (**g**) tertiary carbon emissions in the HD-HI zone.

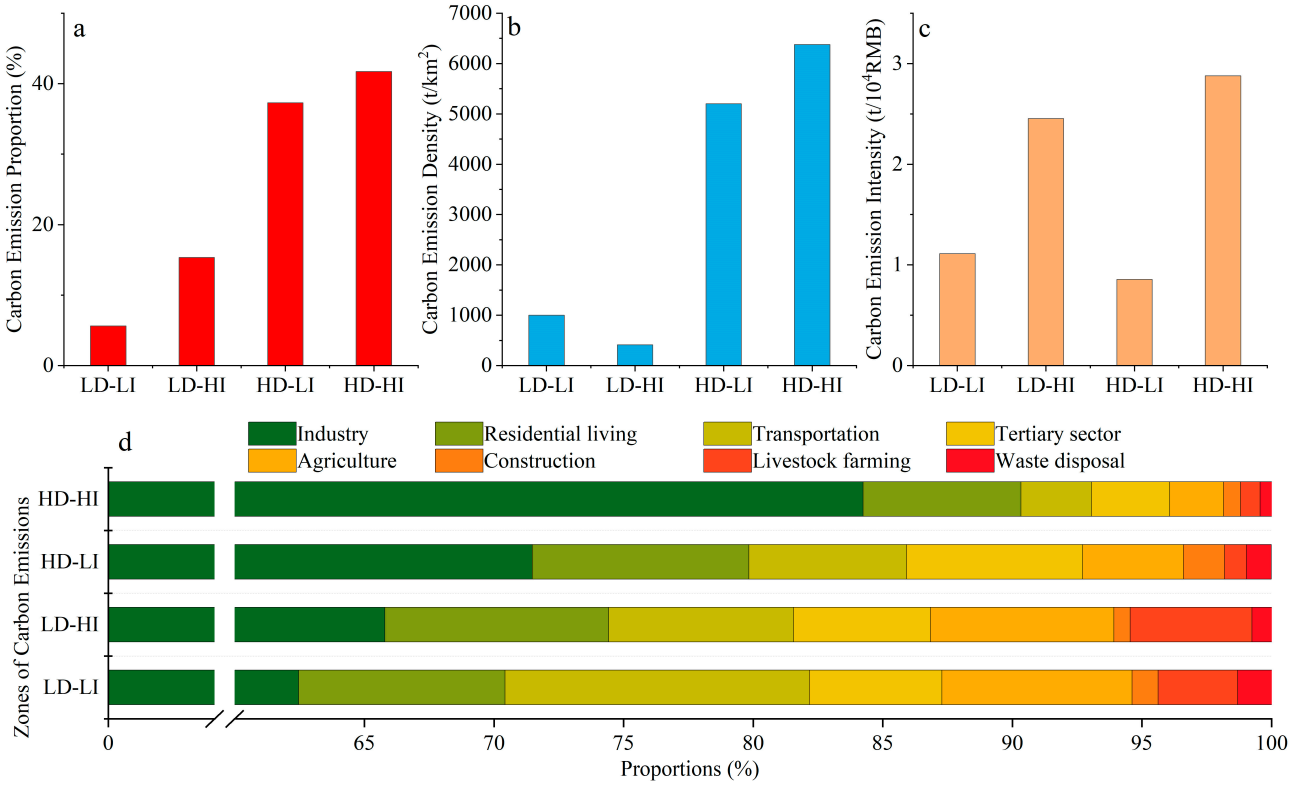

Figure 9. Characteristics of carbon emissions in different zones: (**a**) proportions of total carbon emissions; (**b**) carbon emission density; (**c**) carbon emission intensity; (**d**) proportions of total carbon emissions in each zone attributed to each carbon-emitting sector.

Industry has been identified as the predominant source of carbon emissions across the four emission zones, significantly influencing both carbon emission density and intensity (Figure 9d). Notably, the proportion of industrial carbon emissions in the HD zones is markedly higher than in the LD zones, with the HD-HI zone exhibiting an exceptional share of 84.24% (Figure 8b,c). This zone, primarily encompassing provinces such as Shanxi, Hebei, Shandong, and Liaoning, is characterized by the dominance of heavy industries, including steel, cement, and chemical manufacturing. These sectors are highly energy-intensive, relying extensively on fossil fuels for production processes, which results in substantial carbon emissions due to their large-scale operations and high energy consumption. In contrast, the LD zone, with a relatively lower level of industrial development, exhibits a smaller proportion of carbon emissions from industry. However, industrial activities still contribute to carbon emissions in these regions. In the LD-LI zone, despite a smaller overall industrial scale compared to the HD zones, specific industries continue to play a significant role in carbon emissions.

Beyond industry, other sectors also exhibit distinct differences in carbon emission patterns, largely influenced by the unique industrial structures and socio-economic characteristics of each zone. In the LD-LI zone, transportation accounts for 11.74% of total carbon emissions. This is largely attributed to the region's relatively sparse urban layout and underdeveloped public transportation infrastructure, leading to increased reliance on private vehicles for commuting and the transportation of goods over longer distances, thereby elevating carbon emissions from the transportation sector (Figure 8d). Additionally, agriculture contributes 7.34% of the carbon emissions in this zone, driven by traditional farming practices such as the use of fossil fuel-powered machinery and the application of fertilizers, which release greenhouse gases during decomposition. The rural characteristics of the LD-LI zone, with a significant portion of the population engaged in

agriculture, further emphasize the role of this sector in overall carbon emissions (Figure 8e). In the LD-HI zone, residential living contributes 8.64% of carbon emissions, which can be attributed to several factors (Figure 8f). The colder climate in certain areas of this region results in higher energy demand for heating during winter months. Moreover, the lifestyle and consumption patterns in this zone likely involve elevated energy use for household appliances and other daily activities. In the HD-HI zone, the tertiary sector accounts for 6.79% of total carbon emissions (Figure 8g). The rapid development of the tertiary sector in this region, which includes commercial services and logistics, leads to emissions from various sources. Commercial buildings in urban areas are significant energy consumers, utilizing large amounts of energy for lighting, heating, ventilation, and air conditioning. Additionally, the logistics and transportation services associated with the tertiary sector, such as the movement of goods and people, contribute further to carbon emissions. The high population density and intense economic activity in the HD-HI zone further amplify the carbon emissions associated with the tertiary sector.

4. Discussion

This study provided a more detailed, higher spatial resolution and broader coverage of carbon emission spatial distribution data in China, providing crucial support for developing more accurate and effective carbon reduction strategies, which have not been reported in the scientific literature. This study calculated emissions across eight sectors that encompass nearly all carbon-emitting activities while also accounting for emissions from coal mining, agricultural inputs, rice cultivation, livestock farming, and waste disposal. Notably, this research utilizes more detailed data on the consumption of 40 types of fossil fuels. Furthermore, it elevates the carbon emission analysis to a spatial resolution of 500 m, covering all 360 cities in China except Tibet, Hong Kong, Macao, and Taiwan. In contrast, previous studies, such as those by Cai et al. (2018), included only four sectors [19], while Shan et al. (2022) focused solely on emissions from 17 types of fossil fuels and considered only 275 prefecture-level cities [22]. More comprehensive carbon emission data are essential for formulating cross-sectoral collaborative reduction strategies, balancing regional emission disparities, and achieving refined carbon management. In addition, Cai et al. (2018) found that China's carbon emission hotspot area was in central east China (including Beijing, Tianjin, Liaoning, Hebei, Shanxi, Shandong, Henan, Jiangsu, and Anhui) [19]. Shan et al. (2022) found that Tangshan, Tianjin, Shanghai, Suzhou, Handan, and Chongqing were six of the top ten locations for total carbon emissions [22]. These results were consistent with the findings of our study. On the other hand, our study also showed a good correlation with the total carbon emission results of CCG ($R^2 = 0.7047$) (Figure 10).

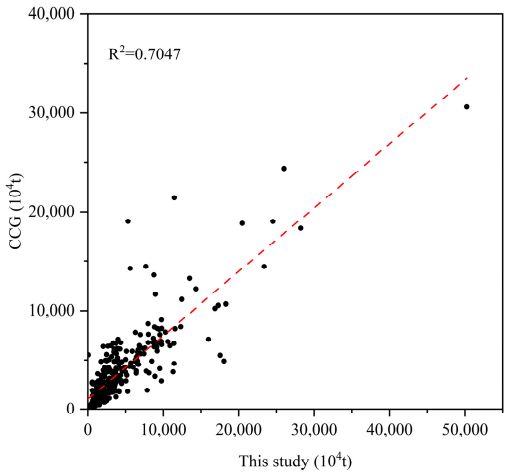

Figure 10. Comparison of total carbon emission values in China estimated by this study and CCG.

Significant differences in carbon emissions exist across regions, closely linked to local policies, stages of economic development, and land use characteristics. For instance, economically developed HD-HI regions tend to have higher emissions due to industrial concentration and high energy consumption, whereas LD-LI regions, dominated by agriculture or with low levels of industrialization, typically exhibit lower total emissions. Exploring these relationships in greater depth provides valuable insights for developing regional and targeted emission reduction policies. However, this study has certain limitations in data sources and methodology that may influence the interpretation of regional differences. For example, emissions from certain sectors might be underestimated due to incomplete data, while spatial data distribution inconsistencies could either exaggerate or downplay regional disparities. Additionally, the lack of historical carbon emission data limits the analysis of dynamic changes across regions, making it difficult to assess long-term trends or the effectiveness of mitigation policies. Future research should incorporate more comprehensive historical data and employ refined spatial analysis methods to better understand regional carbon emission disparities and their underlying causes.

4.1. Strengths and Uncertainty in Carbon Emission Estimation

Carbon emissions in China have received extensive attention from the rest of the world. Accurately estimating carbon emissions is dependent not only on identifying emission sectors but also on access to data resources. Our study showed obvious advantages in the spatial resolution of carbon emissions, especially in the identification of carbon emission hotspots. As shown in Figure 11, six large areas in Shanghai with carbon emissions exceeding 50×10^3 t/grid cell were accurately identified in our study: industrial and logistics center park in Baoshan District (Figure 11b), Shanghai Hongqiao International Airport (Figure 11c), Centralized chemical industry park (Figure 11d), Shanghai Port Container Waigaoqiao Marina (Figure 11e), Shanghai Pudong International Airport (Figure 11f), and Shanghai Disney Resort (Figure 11g). These areas all involve significant energy consumption and carbon emissions in their operations, especially Shanghai Hongqiao International Airport and Shanghai Pudong International Airport, which both rank among the top ten airports in China in terms of passenger traffic.

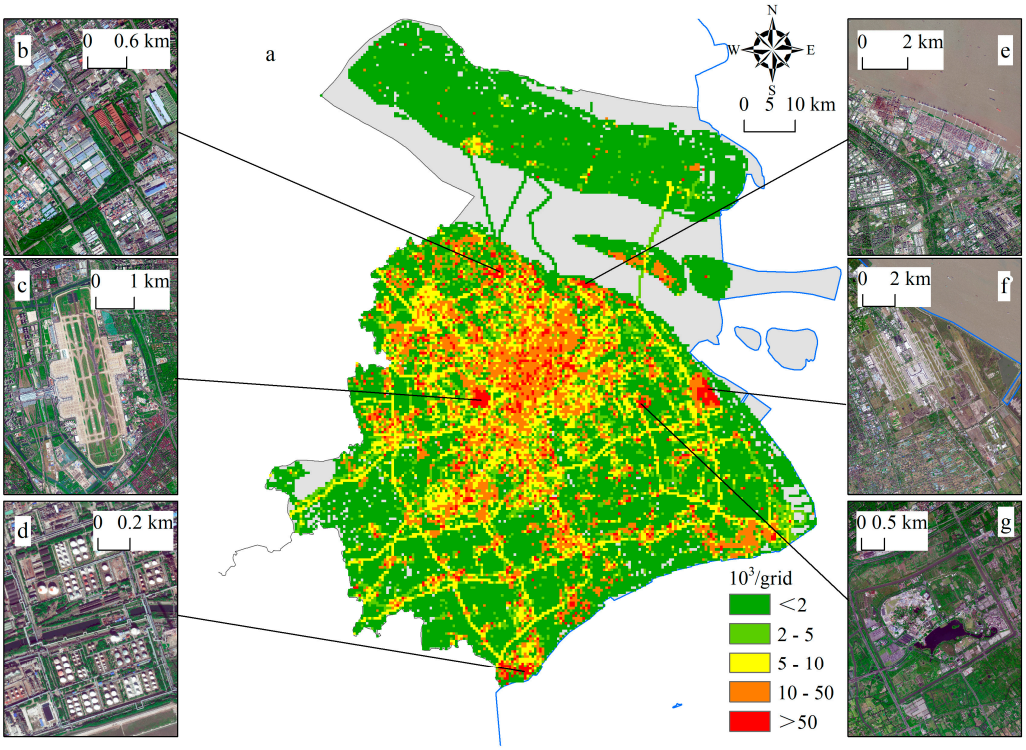

Figure 11. Example of carbon emission precision in Shanghai: (**a**) carbon emissions in Shanghai City; (**b**–**g**) true-color images (sourced from Baidu Maps): (**b**) industrial and logistics center park in Baoshan District; (**c**) Shanghai Hongqiao International Airport; (**d**) centralized chemical industry park; (**e**) Shanghai Port Container Waigaoqiao Marina; (**f**) Shanghai Pudong International Airport; (**g**) Shanghai Disney Resort.

In general, the calculation results of this study reflected the amount and spatial distribution of China's carbon emissions more accurately. However, the following limitations and uncertainties associated with our study should be considered:

(1) Obtaining detailed data at the prefecture-level was challenging. Since some prefecture-level city-level statistical data were not published in the statistical year book, this study used available proxy data (such as per capita income and grain production) to allocate provincial-level data to prefecture levels. For instance, among 26 provinces and autonomous regions, 19 disclosed fertilizer usage at the prefecture level in 2020, while seven did not stop the usage. Grain output is affected by the use of chemical fertilizers to a certain extent. Therefore, this study allocated provincial fertilizer usage totals to prefecture levels using grain production as proxy data. However, the limited availability of relevant data in statistical yearbooks for some provinces, coupled with the fact that most prefecture-level cities do not publish statistical yearbooks or include only partial data, resulted in certain cities relying heavily on proxy data for carbon emission calculations. This reliance introduced notable limitations and potential uncertainties in the carbon emission estimates. Additionally, the data in statistical yearbooks is predominantly derived from departmental reports, meaning that some figures may be based on estimations rather than actual measurements. For example, industrial production data are often derived from reports submitted by medium and large-scale industries, while production data from smaller processing facilities are typically excluded. This omission could adversely affect the accuracy of carbon emission calculations, especially in regions with a high prevalence of small-scale industries.

In future research, governments and statistical agencies should prioritize the establishment of more detailed data collection systems that account for contributions from smaller industries and provide more granular reporting at the county level. Strengthening

coordination among different administrative levels can further enhance data availability and accuracy. (2) The temporal precision of high-resolution spatial data also constrained the calculation and spatial representation of carbon emissions, especially the POI data. Large-scale reporting of POI data in China generally began in 2010 [44], resulting in a relatively short study period for the spatialization of carbon emissions using POI data. This limitation hinders the ability to conduct long-term carbon emission monitoring. Furthermore, some POI entries may contain errors, such as incorrect location tagging or misclassification of industries. Additionally, certain areas may suffer from missing POI data, particularly in remote regions or for small enterprises and establishments that might not be recorded, leading to gaps or inaccuracies in spatialized carbon emission results. POI data updates are not real-time, and as urban development and industrial restructuring progress, new emission sources continuously emerge, while older sources may disappear or change in scale. The coverage of POI data also varies significantly across regions. In urban centers and densely populated commercial areas, POI data are rich and detailed, offering a comprehensive reflection of various emission sources. However, in rural areas, remote regions, or economically underdeveloped areas, the density and richness of POI data are substantially lower, potentially omitting many emission sources. This disparity compromises the completeness and accuracy of spatialized carbon emission results across different geographic regions. Moreover, POI data only indicate the location of emission sources but do not provide information on their scale. Consequently, within the same prefecture-level city, emission sources of varying scales within the same industry are treated equally, which adversely impacts the accuracy of the calculation results. In future research, it is possible to consider cooperating with platforms that provide POI data to speed up the update frequency of POI data. Additionally, it would be beneficial to incorporate descriptive fields related to the scale of carbon emissions within the POI data, such as production scale, building area, and employee numbers. By collecting and organizing this information, a more accurate assessment of the emission intensity of sources of varying scales can be achieved.

4.2. Spatial Variation in Carbon Emissions in China

There were obvious spatial distribution differences in carbon emissions in China, especially the carbon emission density and economic carbon intensity (see Section 3.2). Carbon emissions are affected by multiple factors, such as population, GDP, and industrial structure [49]. Analysis of the causes of the spatial distribution pattern of carbon emissions in China can provide a basis for formulating precise emission reduction recommendations.

The spatial distribution of China's population (Figure 12a) and GDP (Figure 12b) in 2020 both had obvious distribution trends of higher in the southeast and lower in the northwest, which is consistent with the spatial distribution pattern of carbon emissions. These maps show that the distribution of carbon emissions was largely affected by population and GDP, and population ($R^2 = 0.4748$) was more highly correlated with carbon emissions than GDP ($R^2 = 0.4040$) (Figure 12c). However, both population and GDP had a limited impact on carbon emissions within China as a whole, so we conducted further analysis for different regions (Figure 13). The results showed that compared to the whole of China, the population and GDP of different regions had a higher impact on carbon emissions, and the impact of GDP on carbon emissions was greater than population, especially in the LD-LI area where carbon emissions were more affected by population and GDP, and where the correlation coefficient between GDP and carbon emissions reached 0.9102.

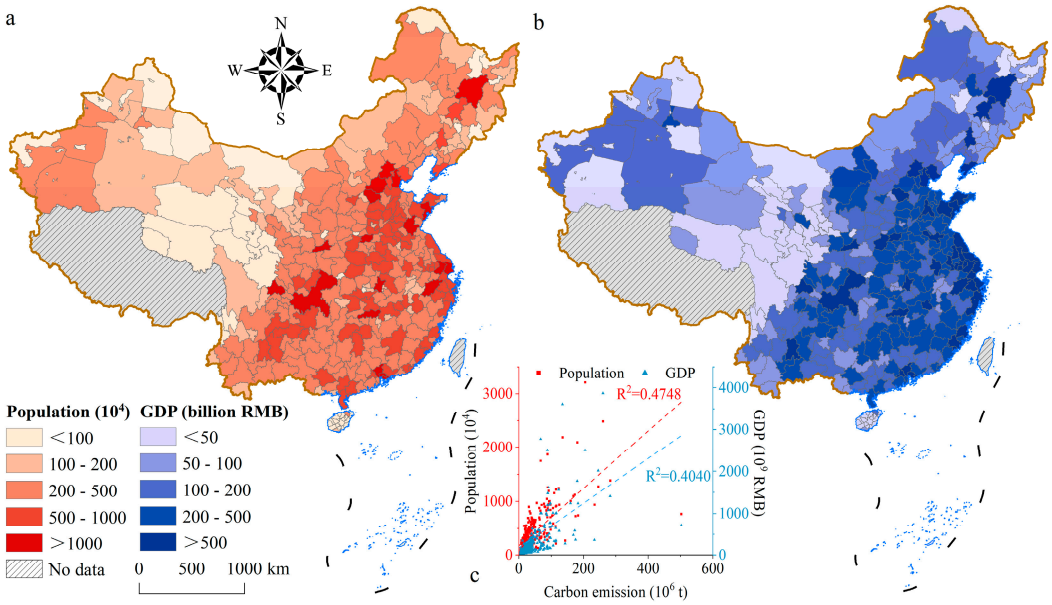

Figure 12. Population and gross domestic product (GDP) of prefecture-level cities in China and their relationship with carbon emissions: (a) Population; (b) GDP; (c) The relationships of carbon emissions with population and GDP.

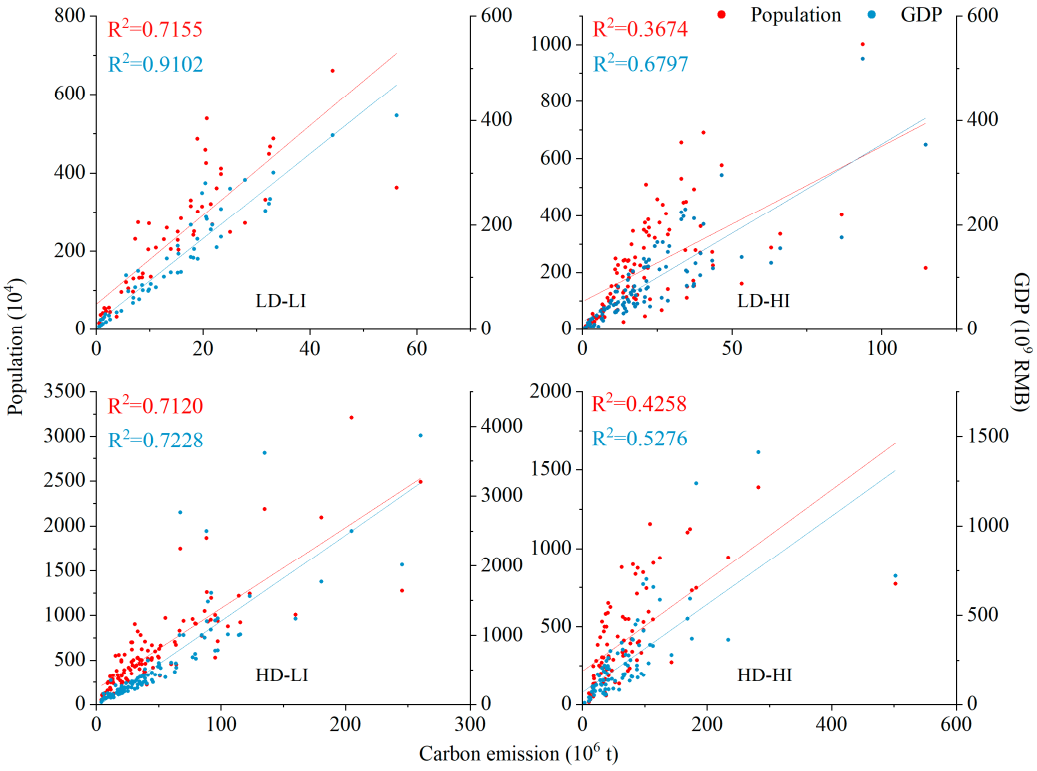

Figure 13. Correlations of carbon emissions with population and gross domestic product (GDP) in different carbon emission density and intensity zones of China.

In view of the different impacts of GDP on carbon emissions in different regions, we further analyzed the impact of industrial structure on carbon emissions. The results in Figure 14 show that the GDP share of the secondary industry in areas with high carbon emission density was significantly higher than in areas with low carbon emission density, while the proportion of primary industry in areas with high carbon emission density was

relatively low, indicating that the secondary industry was the main factor affecting carbon emissions, proving the previous research results.

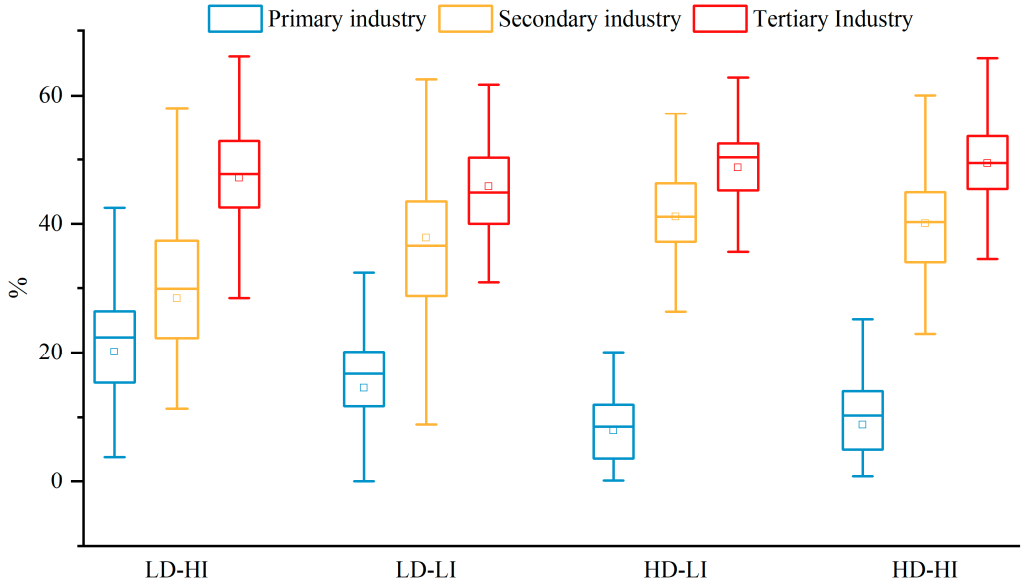

Figure 14. Proportions of gross domestic product (GDP) associated with different industry classifications in different carbon emission density and intensity zones in China (the lower and upper box boundaries indicate the 25th and 75th percentiles; the horizontal line in the box is the mean; the square symbol in the box is the median; the lower and upper whiskers indicate the minimum and maximum values).

It is worth noting that the industrial structures of the HD-LI zone and the HD-HI zone were similar, but they showed huge differences in economic carbon intensity. Therefore, we compared the secondary industrial structure of three provinces in the HD-HI zone (Shanxi, Liaoning, and Hebei) and three provinces in the HD-LI zone (Jiangsu, Henan, and Hubei) (Figure 15). The results showed that the heavy industry operating cost ratio of the three provinces in the HD-HI zone was significantly higher than in the HD-LI zone, especially in Shanxi Province, where the heavy industry operating cost contributed to 96% of the total industrial operating cost. These results show that the development of heavy industry was the main reason for the high economic carbon intensity in the region.

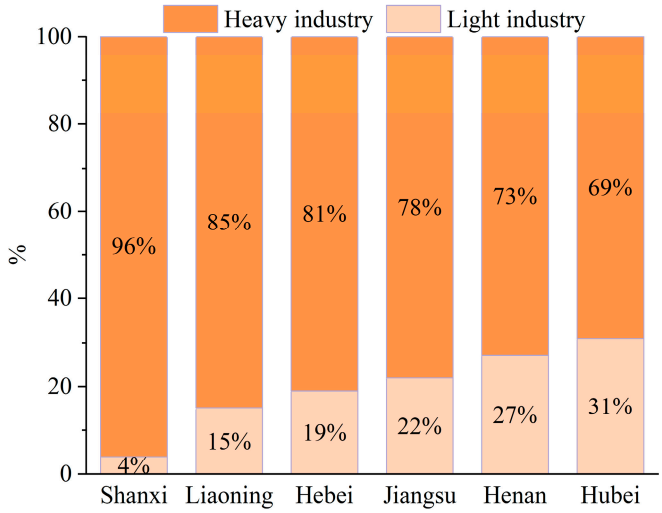

Figure 15. Proportion of operating costs of light industry and heavy industry for six provinces in China.

4.3. Suggestions for Carbon Emission Reduction

Proposing targeted suggestions based on the carbon emission sources in different zones is of great significance in achieving carbon emission reduction, but the actual development conditions of different zones should also be considered when making suggestions.

In the HD-HI region, carbon emission density is notably high, ranging from 5200.48 to 6377.09 t/km^2, far surpassing that of the LD regions. This region, located primarily in provinces such as Shanxi, Hebei, Shandong, and Liaoning, relies heavily on heavy industry, including sectors like steel, cement, and fertilizers. As shown in Figure 9c, industrial emissions account for 84.24% of total emissions in this area. The high energy consumption and carbon emissions associated with heavy industry processes result in elevated carbon emission density and economic carbon intensity (2.45–2.88 t/10^4 RMB). Due to the region's energy-intensive industrial structure, economic growth is strongly dependent on carbon emissions. Consequently, policy efforts should focus on encouraging heavy industries to switch to cleaner energy sources, such as natural gas and solar power, while promoting low-carbon materials and energy-efficient technologies. Given the contribution of residential and transportation emissions, improving public transportation systems and promoting low-carbon lifestyles, such as using energy-efficient appliances and building materials, should also be prioritized.

The HD-LI region has a lower carbon emission density, ranging from 411.61 to 1002.07 t/km^2. While the emission density is relatively lower than in the HD-HI region, the economic carbon intensity (0.86–1.11 t/10^4 RMB) remains relatively high. This is primarily due to the region's reliance on light industry and the tertiary sector. The region's industrial structure is more optimized, particularly in light industry and services, which have contributed to more effective control of carbon emissions. In this region, policy should encourage light industry companies to upgrade their technologies and improve energy efficiency in production processes, with financial incentives such as tax breaks and subsidies for adopting advanced energy-saving equipment. At the same time, energy efficiency standards should be implemented in the service sector, including commercial buildings and hotels, which would reduce energy consumption and carbon emissions. Moreover, promoting the decarbonization of public transportation by increasing the use of electric buses and optimizing traffic networks can significantly reduce emissions. Public education campaigns that encourage low-carbon lifestyles will also help raise awareness and further reduce the region's carbon footprint.

In the LD-HI region, emissions from agriculture and transportation make up a substantial share of total carbon emissions, presenting a significant challenge for low-carbon development. Despite the region's relatively low carbon emission density, its economic carbon intensity is higher, primarily due to the high proportion of emissions from agriculture (7.34%) and transportation (11.74%). Traditional agricultural practices, which rely heavily on chemical fertilizers and machinery, contribute to significant emissions. Additionally, the region's scattered urban layout and inadequate transportation infrastructure exacerbate the carbon emissions from the transport sector. Furthermore, residential emissions also contribute to the total carbon output. Therefore, policies should focus on promoting sustainable agricultural practices, such as organic farming, precision fertilization, and the adoption of low-carbon production technologies. Simultaneously, optimizing urban and transportation planning to reduce travel distances and congestion and promoting the use of green transportation options, such as electric vehicles, will help lower emissions. Public awareness campaigns, especially through

schools and community-based programs, should encourage low-carbon living and the adoption of energy-saving habits, which will further support emissions reduction efforts.

The LD-LI region, while having lower carbon emission density and economic carbon intensity, still faces challenges due to its relatively single-industrial structure, which relies on traditional sectors such as agriculture and small-scale industry. In this region, emissions from industry, agriculture, and transportation each represent a significant share of total emissions, indicating that reducing emissions while promoting economic development remains a challenging task. To address this, policies should foster industrial synergy by integrating agriculture, industry, and services, such as through the development of agro-processing industries, which would increase the added value of agricultural products and drive low-carbon transformation in related sectors.

In conclusion, policymakers should adopt differentiated carbon reduction strategies based on the unique emission characteristics of each region. For regions dominated by heavy industry, efforts should focus on energy substitution and technological innovation; in regions where agriculture and transportation emissions are prominent, emphasis should be placed on agricultural emissions reduction and transportation system optimization; and in areas with lower carbon efficiency, promoting industrial synergy and green transformation should be the priority. Future research could further assess the effectiveness of these policies and provide additional insights to optimize carbon reduction strategies.

5. Conclusions

In this study, carbon emissions from a larger scope and more sources in 2020 were estimated by using data from 360 prefecture-level cities in China that included 500-m resolution data for CO_2 and CH_4 emissions in eight carbon-emitting sectors (agriculture, industry, livestock farming, construction, transportation, tertiary sector, residential living, and waste disposal). We then divided China into four carbon emission density and intensity zones, LD-LI, LD-HI, HD-LI, and HD-HI, and analyzed the sources of carbon emissions in different regions. China's total carbon emissions in 2020 were 146.00×10^8 t, and carbon emissions in the southeastern region were significantly higher than carbon emissions in the northwest. The main source of China's carbon emissions was industry, accounting for 75.42% of total carbon emissions. Therefore, adjusting the industrial structure and optimizing industrial production technology will be important tasks for China in order to reduce emissions for a long time to come. Residential living and transportation contributed to 7.44% and 5.16%, respectively, of total carbon emissions. Implementing energy-saving measures in daily life and promoting environmentally friendly transportation methods will be essential actions for reducing carbon emissions. There was obvious heterogeneity in the carbon emission characteristics of different zones, so proposing targeted opinions based on the sources and development levels of carbon emissions in different zones is of great significance to reducing carbon emissions. From a global perspective, the methodology and findings of this study are not only relevant to China but also provide a valuable model for other nations with significant regional heterogeneity in carbon emissions. Countries undergoing rapid industrialization and urbanization can draw upon this research to better understand their emission patterns and formulate region-specific strategies for sustainable development. To further advance the understanding and management of carbon emissions, future research could focus on continuous temporal monitoring to capture dynamic changes over time, offering more comprehensive insights into emission trends. Moreover, leveraging emerging technologies such as high-resolution satellite imagery and machine learning algorithms could significantly enhance data accuracy and spatial precision. These advancements would enable more detailed assessments of emission sources and patterns, refine emission inventories, and support the effective implementation of tailored carbon reduction strategies. Ultimately, such efforts would contribute to global initiatives aimed at addressing climate change.

Author Contributions: Conceptualization, J.G., J.L., and G.D.; methodology, J.G., J.S., and Y.Q.; software, J.G., J.L., and G.D.; validation, J.G.; resources, J.G. and Y.Q.; data curation, J.G.; writing—original draft preparation, J.G.; writing—review and editing, J.G., Y.Q., X.W., and M.K.S.; visualization, J.G.; funding acquisition, Y.Q. All authors have read and agreed to the published version of the manuscript.

Funding: The study was financially supported by the China National Science Fund Program (No. 42277310) and The Natural Science Basic Research Program of Shaanxi (No. 2022PT-28).

Data Availability Statement: The datasets generated during and/or analyzed during the current study are available from the corresponding author upon reasonable request.

Acknowledgments: We thank all researchers, graduate students involved in data collection, and reviewers for their contributions.

Conflicts of Interest: The authors declare that they have no known competing financial interests or personal relationships that could have influenced the work reported in this paper.

Abbreviations

The following abbreviations are used in this manuscript:

CO_2	Carbon dioxide
CH_4	Methane
LD-LI	Low carbon emission density and low economic carbon intensity zone
LD-HI	Low carbon emission density and high economic carbon intensity zone
HD-LI	High carbon emission density and low economic carbon intensity zone
HD-HI	High carbon emission density and high economic carbon intensity zone

Appendix A

Table A1. Selected carbon-emitting sectors and proportional quantities of industrial POI data.

Industrial Sector	Proportion	Industrial Sector	Proportion
Mining and washing of coal	0.20%	Manufacture of medicines	2.39%
Extraction of petroleum and natural gas	0.02%	Manufacture of chemical fiber	0.26%
Mining of ferrous metal ores	0.01%	Manufacture of rubber and plastic	5.19%
Mining of non-ferrous metal ores	0.02%	Manufacture of non-metallic mineral products	9.95%
Mining and processing of non-metal ores	0.53%	Smelting and pressing of ferrous metals	2.78%
Support activities for mining	0.07%	Smelting and pressing of non-ferrous metals	0.89%
Processing of food from agricultural products	2.59%	Manufacture of metal products	11.25%
Manufacture of food	4.70%	Manufacture of general-purpose machinery	9.92%
Manufacture of liquor, beverages, and refined tea	2.81%	Manufacture of special-purpose machinery	3.93%
Manufacture of tobacco	0.18%	Manufacture of automobiles	2.05%
Manufacture of textile	4.64%	Manufacture of railway, ship, aerospace, and other transport Equipment	0.43%
Manufacture of textiles, wearing apparel, and accessories	5.00%	Manufacture of electrical machinery and apparatus	7.03%
Manufacture of leather, fur, feather and its products, footwear	1.68%	Manufacture of computers, communication, and other electronic equipment	3.52%
Processing of timber, manufacture of wood, bamboo, rattan, palm, and straw products	2.20%	Manufacture of measuring instruments and machinery	0.46%
Manufacture of furniture	2.63%	Manufacture of other products	0.06%
Manufacture of paper and paper products	1.78%	Utilization of waste resources	0.88%
Printing, reproduction of recording media	1.92%	Repair service of metal products, machinery, and equipment	0.09%
Manufacture of articles for culture, education, arts and crafts, sport and entertainment activities	1.95%	Production and supply of electric power and thermal power	1.54%
Processing of petroleum, coking, processing of nuclear fuel	0.91%	Production and supply of gas	0.38%
Manufacture of raw chemical materials and chemical products	2.77%	Production and supply of water	0.39%

Table A2. Data levels and processing for non-spatial data.

Statistical Data Type	Data Level	Proxy Data
Agricultural energy consumption	Provincial	Grain production
Agricultural input materials	Provincial, prefecture-level city	Grain production
Rice cultivation area	Provincial	Rice production
Number of free-range livestock	Provincial, prefecture-level city	Production of beef, lamb, and pork
Number of livestock raised in confinement	Provincial, prefecture-level city	Production of beef, lamb, and pork
Industrial energy consumption	Provincial	Operating costs of various industries
Raw coal production	Prefecture-level city	-

Industrial product output	Provincial, prefecture-level city	Number of various types of factories
Construction energy consumption	Provincial	Construction area of buildings
Transportation energy consumption	Provincial	Road mileage
Urban residential energy consumption	Provincial	Urban resident income levels
Rural residential energy consumption	Provincial	Rural resident income levels
Sewage treatment volume	Provincial	-
Waste incineration volume	Provincial	-
Waste landfilling volume	Provincial	-
Wholesale, retail, and catering services energy consumption	Provincial	Total output value of the tertiary sector
Other energy consumption	Provincial	Total output value of the tertiary sector

Table A3. Sources of carbon emission factors for different emission types.

Carbon Emissions Sources	**Description**	**Sources of Carbon Emission Coefficients**
Energy consumption	CO_2 emissions from the consumption of 30 types of energy sources (such as raw coal, crude oil, and natural gas).	[50-52]
Coal mining	CH_4 emissions from coal mining	[45]
Industrial production processes	CO_2 emissions from cement, pig iron, and steel production processes	[50-51]
Agricultural input materials	CO_2 emissions from agricultural input materials, including pesticides, agricultural films, fertilizers, and irrigation	[11-12]
Waste incineration	CO_2 emissions from waste incineration	[50]
Livestock farming	CH_4 emissions from pig, cattle, and sheep farming	[50][50]
Rice cultivation	CH_4 emissions from rice cultivation	[50][50]
Sewage treatment	CH_4 emissions from sewage treatment	[50][50]
Landfilling of waste	CH_4 emissions from waste landfilling	[50][50]

Table A4. Proxy data of different carbon emission types.

Carbon Emission Source	Data Type	Proxy Data	Land Use Type
Industrial energy consumption	Point	POI for 40 industrial sectors	-
Coal mining		POI for coal mining industries	-
Industrial production process		POI for cement, pig iron, and steel production industries	-
Livestock farming		POI for large-scale pig, cattle, and sheep farming facilities	-
Waste disposal		POI for sewage treatment plants, landfill sites, and waste incineration plants	-
Transportation energy consumption	Line	Maximum traffic volume and road length for different road levels	-
Agricultural energy consumption	Area	Cropland area	Farmland
Agricultural input materials		Cropland area	Farmland
Rice cultivation		Paddy field area	Paddy field
Energy consumption in construction		Nighttime light data	Other construction land
Energy consumption in tertiary sector		Nighttime light data	Other construction land
Urban residential living energy consumption		Population density in urban areas	Urban constructive land
Rural residential living energy consumption		Population density in rural areas	Rural constructive land.
Free-range livestock farming		Rural population density	Rural constructive land

References

1. Li, G.P.; Yuan, Y. Impact of regional development on carbon emission: Empirical evidence across countries. *Chin. Geogr. Sci.* **2014**, *24*, 499–510. https://doi.org/10.1007/s11769-014-0710-5.
2. Xu, G.H.; Ge, Q.S.; Gong, P.; Fang, X.Q.; Cheng, B.B.; He, B.; Luo, Y.; Xu, B. Societal response to challenges of global change and human sustainable development. *Chin. Sci. Bull.* **2013**, *58*, 3161–3168. https://doi.org/10.1007/s11434-013-5947-3.
3. Li, Y.; Yao, S.; Jiang, H.; Wang, H.; Ran, Q.; Gao, X.; Ding, X.; Ge, D. Spatial-Temporal Evolution and Prediction of Carbon Storage: An Integrated Framework Based on the MOP–PLUS–InVEST Model and an Applied Case Study in Hangzhou, East China. *Land* **2022**, *11*, 2213. https://doi.org/10.3390/land11122213.
4. Shahbaz, M.; Zakaria, M.; Shahzad, S.J.H.; Mahalik, M.K. The energy consumption and economic growth nexus in top ten energy-consuming countries: Fresh evidence from using the quantile-on-quantile approach. *Energy Econ.* **2018**, *71*, 282–301. https://doi.org/10.1016/j.eneco.2018.02.023.
5. Shan, Y.L.; Guan, D.B.; Zheng, H.R.; Ou, J.M.; Li, Y.; Meng, J.; Mi, Z.F.; Liu, Z.; Zhang, Q. Data Descriptor: China CO_2 emission accounts 1997–2015. *Sci. Data* **2018**, *5*, 170201. https://doi.org/10.1038/sdata.2017.201.
6. Shan, Y.L.; Huang, Q.; Guan, D.B.; Hubacek, K. China CO_2 emission accounts 2016–2017. *Sci. Data* **2020**, *7*, 54. https://doi.org/10.1038/s41597-020-0393-y.
7. He, J.-K. China's INDC and non-fossil energy development. *Adv. Clim. Change Res.* **2015**, *6*, 210–215. https://doi.org/10.1016/j.accre.2015.11.007.
8. Normile, D. China's bold climate pledge earns praise-but is it feasible? *Science* **2020**, *370*, 17–18.
9. Pan, X.Z.; Wang, L.N.; Chen, W.Y.; du Pont, Y.R.; Clarke, L.; Yang, L.; Wang, H.L.; Lu, X.; He, J.K. Decarbonizing China's energy system to support the Paris climate goals. *Sci. Bull.* **2022**, *67*, 1406–1409. https://doi.org/10.1016/j.scib.2022.05.020.
10. Guan, Y.R.; Shan, Y.L.; Huang, Q.; Chen, H.L.; Wang, D.; Hubacek, K. Assessment to China's Recent Emission Pattern Shifts. *Earths Future* **2021**, *9*, e2021EF002241. https://doi.org/10.1029/2021EF002241.
11. Moucheng, L.; Lun, Y. Spatial pattern of China's agricultural carbon emission performance. *Ecol. Indic.* **2021**, *133*, 108345. https://doi.org/10.1016/j.ecolind.2021.108345.
12. Wang, G.F.; Liao, M.L.; Jiang, J. Research on Agricultural Carbon Emissions and Regional Carbon Emissions Reduction Strategies in China. *Sustainability* **2020**, *12*, 2627. https://doi.org/10.3390/su12072627.

13. Zhang, P.; Hu, J.; Zhao, K.X.; Chen, H.; Zhao, S.D.; Li, W.W. Dynamics and Decoupling Analysis of Carbon Emissions from Construction Industry in China. *Buildings* **2022**, *12*, 257. https://doi.org/10.3390/buildings12030257.
14. Qu, J.S.; Liu, L.N.; Zeng, J.J.; Zhang, Z.Q.; Wang, J.P.; Pei, H.J.; Dong, L.P.; Liao, Q.; Maraseni, T. The impact of income on household CO_2 emissions in China based on a large sample survey. *Sci. Bull.* **2019**, *64*, 351–353. https://doi.org/10.1016/j.scib.2019.02.001.
15. Gao, P.; Yue, S.J.; Chen, H.T. Carbon emission efficiency of China's industry sectors: From the perspective of embodied carbon emissions. *J. Cleaner Prod.* **2021**, *283*, 124655. https://doi.org/10.1016/j.jclepro.2020.124655.
16. Wang, Y.; Yang, H.X.; Sun, R.X. Effectiveness of China's provincial industrial carbon emission reduction and optimization of carbon emission reduction paths in "lagging regions": Efficiency-cost analysis. *J. Environ. Manage.* **2020**, *275*, 111221. https://doi.org/10.1016/j.jenvman.2020.111221.
17. Guo, M.Y.; Chen, S.L.; Zhang, J.; Meng, J. Environment Kuznets Curve in transport sector?s carbon emission: Evidence from China. *J. Cleaner Prod.* **2022**, *371*, 133504. https://doi.org/10.1016/j.jclepro.2022.133504.
18. Lin, B.Q.; Lei, X.J. Carbon emissions reduction in China's food industry. *Energy Policy* **2015**, *86*, 483–492. https://doi.org/10.1016/j.enpol.2015.07.030.
19. Cai, B.F.; Liang, S.; Zhou, J.; Wang, J.N.; Cao, L.B.; Qu, S.; Xu, M.; Yang, Z.F. China high resolution emission database (CHRED) with point emission sources, gridded emission data, and supplementary socioeconomic data. *Resour. Conserv. Recycl.* **2018**, *129*, 232–239. https://doi.org/10.1016/j.resconrec.2017.10.036.
20. Cai, B.F.; Wang, X.Q.; Huang, G.H.; Wang, J.N.; Cao, D.; Baetz, B.W.; Liu, L.; Zhang, H.; Fenech, A.; Liu, Z. Spatiotemporal Changes of China's Carbon Emissions. *Geophys. Res. Lett.* **2018**, *45*, 8536–8546. https://doi.org/10.1029/2018GL079564.
21. Kong, H.J.; Shi, L.F.; Da, D.; Li, Z.J.; Tang, D.C.; Xing, W. Simulation of China's Carbon Emission based on Influencing Factors. *Energies* **2022**, *15*, 3272. https://doi.org/10.3390/en15093272.
22. Shan, Y.L.; Guan, Y.R.; Hang, Y.; Zheng, H.R.; Li, Y.X.; Guan, D.B.; Li, J.S.; Zhou, Y.; Li, L.; Hubacek, K. City-level emission peak and drivers in China. *Sci. Bull.* **2022**, *67*, 1910–1920. https://doi.org/10.1016/j.scib.2022.08.024.
23. Wang, J.N.; Cai, B.F.; Zhang, L.X.; Cao, D.; Liu, L.C.; Zhou, Y.; Zhang, Z.S.; Xue, W.B. High Resolution Carbon Dioxide Emission Gridded Data for China Derived from Point Sources. *Environ. Sci. Technol.* **2014**, *48*, 7085–7093. https://doi.org/10.1021/es405369r.
24. Olivier, J.G.J.; Van Aardenne, J.A.; Dentener, F.J.; Pagliari, V.; Ganzeveld, L.N.; Peters, J.A.H.W. Recent trends in global greenhouse gas emissions:regional trends 1970–2000 and spatial distributionof key sources in 2000. *Environ. Sci.* **2005**, *2*, 81–99. https://doi.org/10.1080/15693430500400345.
25. Oda, T.; Maksyutov, S. A very high-resolution (1 km×1 km) global fossil fuel CO_2 emission inventory derived using a point source database and satellite observations of nighttime lights. *Atmos. Chem. Phys.* **2011**, *11*, 543–556. https://doi.org/10.5194/acp-11-543-2011.
26. Chuai, X.W.; Feng, J.X. High resolution carbon emissions simulation and spatial heterogeneity analysis based on big data in Nanjing City, China. *Sci. Total Environ.* **2019**, *686*, 828–837. https://doi.org/10.1016/j.scitotenv.2019.05.138.
27. Zhao, Y.-c.; Tian, Y.; Zhang, Q.-p.; Jiang, L.-y.; Wang, Q. Carbon emission reduction potential of land use in typical alpine meadow region in China. *Sustain. Prod. Consum.* **2025**, *53*, 64–77. https://doi.org/10.1016/j.spc.2024.11.029.
28. Xia, C.; Zhang, J.; Zhao, J.; Xue, F.; Li, Q.; Fang, K.; Shao, Z.; Zhang, J.; Li, S.; Zhou, J. Exploring potential of urban land-use management on carbon emissions—A case of Hangzhou, China. *Ecol. Indic.* **2023**, *146*, 109902. https://doi.org/10.1016/j.ecolind.2023.109902.
29. Dong, Z.; Xia, C.; Fang, K.; Zhang, W. Effect of the carbon emissions trading policy on the co-benefits of carbon emissions reduction and air pollution control. *Energy Policy* **2022**, *165*, 112998. https://doi.org/10.1016/j.enpol.2022.112998.
30. Long, Z.; Zhang, Z.L.; Liang, S.; Chen, X.P.; Ding, B.W.P.; Wang, B.; Chen, Y.B.; Sun, Y.Q.; Li, S.K.; Yang, T. Spatially explicit carbon emissions at the county scale. *Resour. Conserv. Recycl.* **2021**, *173*, 105706. https://doi.org/10.1016/j.resconrec.2021.105706.
31. Cai, B.F.; Zhang, L.X. Urban CO_2 emissions in China: Spatial boundary and performance comparison. *Energy Policy* **2014**, *66*, 557–567. https://doi.org/10.1016/j.enpol.2013.10.072.
32. Cai, B.F.; Guo, H.X.; Ma, Z.P.; Wang, Z.X.; Dhakal, S.; Cao, L.B. Benchmarking carbon emissions efficiency in Chinese cities: A comparative study based on high-resolution gridded data. *Appl. Energy* **2019**, *242*, 994–1009. https://doi.org/10.1016/j.apenergy.2019.03.146.
33. Chen, Q.L.; Cai, B.F.; Dhakal, S.; Pei, S.; Liu, C.L.; Shi, X.P.; Hu, F.F. CO_2 emission data for Chinese cities. *Resour. Conserv. Recycl.* **2017**, *126*, 198–208. https://doi.org/10.1016/j.resconrec.2017.07.011.

34. Gurney, K.R.; Patarasuk, R.; Liang, J.M.; Song, Y.; O'Keeffe, D.; Rao, P.; Whetstone, J.R.; Duren, R.M.; Eldering, A.; Miller, C. The Hestia fossil fuel CO_2 emissions data product for the Los Angeles megacity (Hestia-LA). *Earth Syst. Sci. Data* **2019**, *11*, 1309–1335. https://doi.org/10.5194/essd-11-1309-2019.
35. Wang, Y. Spatial-Temporal Evolution and Scenario Simulation of Territorial Spatial Carbon Emission in Wuhan City. Ph.D. Thesis. China University of Geosciences: Wuhan, China, **2022**.
36. National Bureau of Statistics of China. China Energy Statistical Yearbook. *China Statistics Press*: Beijing,China, **2021**.
37. China Statistics Press. China Population Census Yearbook 2020. Availabe online: https://www.stats.gov.cn/sj/pcsj/rkpc/7rp/zk/indexch.htm (accessed on 9 April 2023).
38. National Bureau of Statistics of China. China Environmental Statistical Yearbook. *China Statistics Press*: Beijing, China, **2021**.
39. Resource and Environmental Science Data Platform. Availabe online: https://www.resdc.cn/DOI/DOI.aspx?DOIID=54 (accessed on 15 April 2023).
40. Resource and Environmental Science Data Platform. Availabe online: https://www.resdc.cn/DOI/DOI.aspx?DOIID=105 (accessed on 16 April 2023).
41. WorldPop Hub. Availabe online: https://hub.worldpop.org/project/categories?id=3 (accessed on 10 April 2023).
42. Ministry of Natural Resources of China. 2022. Availabe online: http://www.mnr.gov.cn/ (accessed on 10 April 2023).
43. Lu, W.; Tao, C.; Li, H.; Qi, J.; Li, Y. A unified deep learning framework for urban functional zone extraction based on multi-source heterogeneous data. *Remote Sens. Environ.* **2022**, *270*, 112830. https://doi.org/10.1016/j.rse.2021.112830.
44. Zhang, X.Y.; Xie, Y.W.; Jiao, J.Z.; Zhu, W.Y.; Guo, Z.C.; Cao, X.Y.; Liu, J.M.; Xi, G.L.; Wei, W. How to accurately assess the spatial distribution of energy CO2 emissions? Based on POI and NPP-VIIRS comparison. *J. Cleaner Prod.* **2023**, *402*, 136656. https://doi.org/10.1016/j.jclepro.2023.136656.
45. Wang, N. Research on China CMM Emissions and Control Measures Based on Regional Factor Analysis. Ph.D. Thesis. China University of Mining and Technology: Beijing, China,: **2013**.
46. Yan, R.; Chen, M.; Xiang, X.; Feng, W.; Ma, M. Heterogeneity or illusion? Track the carbon Kuznets curve of global residential building operations. *Appl. Energy* **2023**, *347*, 121441. https://doi.org/10.1016/j.apenergy.2023.121441.
47. Goldemberg, J. A note on the effectiveness of the decline of the carbon intensity on carbon emissions. *Energy Policy* **2022**, *171*, 113258. https://doi.org/10.1016/j.enpol.2022.113258.
48. Li, Q.; Peng, K.L.; Cheng, P. Community-Level Urban Green Space Equity Evaluation Based on Spatial Design Network Analysis (sDNA): A Case Study of Central Wuhan, China. *Int. J. Environ. Res. Public Health* **2021**, *18*, 10174. https://doi.org/10.3390/ijerph181910174.
49. Lu, L.L.; Zhou, L.; Zhang, H.Y.; Weng, Y.Y. The effects of industrial energy consumption on energy-related carbon emissions at national and provincial levels in China. *Energy Sci. Eng.* **2018**, *6*, 371–384. https://doi.org/10.1002/ese3.206.
50. National Development and Reform Commission (NDRC). Guidelines for Provincial Greenhouse Gas Inventory Compilation (Trial). Beijing, China, **2011**.
51. IPCC. 2019 Refinement to the 2006 IPCC Guidelines for National Greenhouse Gas Inventories. Available online: http://www.ipcc.ch/about/preparingreports/ (accessed on 12 April 2023).
52. Ministry of Ecology and Environment of China (MEE). Explanation of the Calculation of CO_2 Baseline Emission Factors for Regional Power Grids in China (2019). Beijing, China, **2020**.